# Opiate Aromatic Pharmacophore Structure−Activity Relationships in CTAP Analogues Determined by Topographical Bias, Two-Dimensional NMR, and Biological Activity Assays

G. Gregg Bonner,[†] Peg Davis,[§] Dagmar Stropova,[§] Sidney Edsall,[§] Henry I. Yamamura,[§] Frank Porreca,[§] and Victor J. Hruby*[,‡]

*Departments of Biochemistry, Chemistry, and Pharmacology, University of Arizona, Tucson, Arizona 85721*

*Received January 14, 1999*

Topographically constrained analogues of the highly $\mu$-opioid-receptor-selective antagonist CTAP (H-D-Phe-c[Cys-Tyr-D-Trp-Arg-Thr-Pen]-Thr-$NH_2$, **1**) were prepared by solid-phase peptide synthesis. Replacement of the D-Phe residue with conformationally biased $\beta$-methyl derivatives of phenylalanine or tryptophan (2*R*,3*R*; 2*R*,3*S*; 2*S*,3*R*; 2*S*,3*S*) yielded peptides that displayed widely varying types of biological activities. In an effort to correlate the observed biological activities of these analogues with their structures, two-dimensional $^1$H NMR and molecular modeling was performed. Unlike the parent (**1**), which is essentially a pure $\mu$ antagonist with weak $\delta$ agonist activities in the MVD bioassay, the diastereomeric $\beta$-MePhe$^1$-containing peptides exhibited simultaneous $\delta$ agonism and $\mu$ antagonism by the (2*R*,3*R*)-containing isomer **2**; $\mu$ antagonism by the (2*R*,3*S*)-containing isomer **3**; weak $\mu$ agonism by the (2*S*,3*R*)-containing isomer **4**; and $\delta$ agonism by the (2*S*,3*S*)-containing isomer **5**. Incorporation of $\beta$-MeTrp isomers into position 1 led to peptides that were $\mu$ antagonists (2*R*,3*R*), **8**; (2*R*,3*S*), **9**, or essentially inactive (<10%) in the MVD and GPI assays (2*S*,3*R*), **10**; (2*S*,3*S*), **11**. Interestingly, in vivo antinociceptive activity was predicted by neither MVD nor GPI bioactivity. When D-Trp was incorporated in position 1, the result (**7**) is a partial, yet relatively potent $\mu$ agonist which also displayed weak $\delta$ agonist activity. Molecular modeling based on 2D NMR revealed that low energy conformers of peptides with similar biological activities had similar aromatic pharmacophore orientations and interaromatic distances. Peptides that exhibit $\mu$ antagonism have interaromatic distances of 7.0−7.9 Å and have their amino terminal aromatic moiety pointing in a direction opposite to the direction that the amino terminus points. Peptides with $\delta$ opioid activity displayed an interaromatic distance of <7 Å and had their amino terminal aromatic moiety pointing in the same direction as the amino terminus.

## Introduction[1]

The development of therapeutically useful painkillers with minimal side effects for severe pain continues to be a major goal. Opiate agonists continue to be used to treat pain but suffer from several liabilities including withdrawal, severe constipation, tolerance, and dependence. Because the affects of opioid ligands may be differentially mediated by the different opiate receptors ($\mu$, $\delta$, $\kappa$), or by simultaneous action at more than one opiate receptor type, the development of high affinity and highly selective ligands remains a major goal. Furthermore, opiate antagonist administration has been shown to have an effect in reducing opiate-related side-effect liability.[2] These factors, when taken together, illustrate the need for selective, high affinity agonists and antagonists for the opiate receptor types and, where possible, the development of ligands that possess agonist activity at one receptor type and antagonist activity at another. It is hoped that these ligands, through simultaneous multiple opiate activity, will lead to therapeutically useful painkillers devoid of side-effect liabilities. Several observations suggest opiate receptor interplay in ligand-induced antinociception. Pretreatment with the non-peptide $\delta$ antagonist naltrindole prevented the development of morphine dependence and tolerance in mice.[2] This suggested that ligands with mixed $\mu$ agonist/$\delta$ antagonist activity, such as H-Tyr-Tic-Phe-Phe-$NH_2$ (TIPP-$NH_2$), may be useful drug leads.[3] Alternatively, ligands may be potent antinociceptive agents due to synergistic agonism at both the $\mu$ and $\delta$ opiate receptor. A conformationally restricted analogue of CTAP (H-D-Tca-c[Cys-Tyr-D-Trp-Arg-Thr-Pen]-Thr-$NH_2$)[4,5] was reported to have a much higher antinociceptive activity than that predicted by its affinity for opiate receptors in radioligand competition assay or in the MVD and GPI assays.[6] The antinociceptive activity of this ligand was blocked by both $\mu$ and $\delta$ antagonists. Hence, it was hypothesized that an interaction between $\mu$ and $\delta$ receptors was responsible for its antinociceptive potency. Finally, it may be possible to develop lead analogues which take advantage of the antinociception resulting from $\delta$ agonism without the side effects associated with morphine administration due to a simultaneous $\mu$ antagonist activity. Analogues with such simultaneous $\mu$ antagonism/$\delta$ agonism have been derived from the $\mu$ antagonist CTAP,[7] from the $\delta$ agonist Deltorphin,[8] and from DPDPE.[9,10]

* To whom correspondence should be addressed. Tel: (520) 621-6332. Fax: (520) 621-8407. E-mail HRUBY@MAIL.ARIZONA.EDU.
[†] Department of Biochemistry.
[‡] Department of Chemistry.
[§] Department of Pharmacology.

10.1021/jm9900218 CCC: $19.00 © 2000 American Chemical Society
Published on Web 01/28/2000

Regardless of which combination of opiate receptor activities will ultimately prove useful in humans, it is still necessary to determine how the structures of the various opioid ligands lead to their observed pharmacological profiles. These sets of structure−activity profiles will be essential in predicting which ligands will yield potent painkilling effects, and which may have side-effect liabilities, as well as determine which features of the ligands must be retained for biological activity as the molecule is modified to make it more biologically available. The elements of opioid peptides hypothesized to be responsible for their activities (the pharmacophores) are a pair of aromatic amino acid residues—one in the amino terminal position, and another in either position three or four. The importance of these pharmacophores is evidenced by their presence in casomorphins, dermorphins, dermenkephalins, deltorphins, enkephalins, dynorphins, endomorphins, and in somatostatin-derived peptides of the CTAP family as well as other synthetic peptides such as DAMGO, TIPP, and ICI-174,864. A free tyramine moiety is almost universally present in opiate peptides, and a phenol moiety is present in non-peptide ligands such as the $\mu$ agonist oxymorphone, $\mu$ antagonist naltrexone, and the $\delta$ antagonist naltrindole. These facts, taken together with the fact that CTAP analogues differing only in the side-chain group stereochemistry of the amino terminal $\beta$-MePhe show varying pharmacological profiles,[7] strongly suggest that the relative orientation and interaromatic distance between the two pharmacophoric aromatic amino acid residue side-chain groups are the principle factors which determine their pharmacological profile.

Several research groups have reported investigations which were intended, at least in part, to determine the interaromatic distances associated with ligands of varying biological activity. The results from these studies have led to different conclusions. One group reported an interaromatic distance of 6.3 Å for the enkephalin-derived analogue DPDPE,[11] whereas another group[12] reported a distance of 4.9−5.6 Å. These values are much less than the >10 Å,[13] 11.5 Å,[9] or 10.9 Å[14] reported elsewhere. The larger separations are in better agreement with the X-ray crystallographic analyses which showed the interaromatic distances in DPDPE to be 15.0 Å and 15.9 Å.[15] The smaller distances are in better agreement with rigid ligands such as naltrindole and SIOM. Similarly conflicting results have been reported for $\mu$-selective peptides. Interaromatic separations of >9 Å[16] and <8 Å[17] have been reported.

In the present paper, we describe the syntheses, biological activity profiles, and structural characterization of analogues of the somatostatin-derived $\mu$ antagonist CTAP which have incorporated in their amino terminal positions, D-Trp or one of the four isomers of the rotamer topography-biasing $\beta$-methyl amino acids $\beta$-MePhe and $\beta$-MeTrp (2*R*,3*R*; 2*R*,3*S*; 2*S*,3*R*; 2*S*,3*S*). In particular, the work describes the synthesis and biological activity determinations of five new analogues (**2**, **3**, **4**, **5**, and **7**). Two-dimensional NMR studies of these five analogues, as well as of four other previously reported[7] analogues (**8**, **9**, **10**, **11**), were performed. These data and NMR-derived computer-aided molecular modeling were used to form a comprehensive structure−activity analysis for all the analogues including others

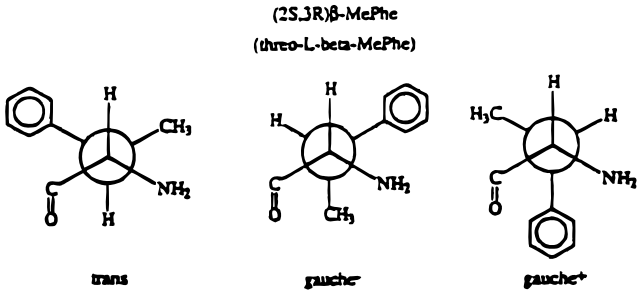


**Figure 1.** Newman projections of the three low energy rotamers of (2*S*,3*R*)$\beta$-MePhe.

previously reported in the literature. Unusual amino acids with $\beta$-methyl substituents have been incorporated into several classes of opioid peptides including enkephalins,[9,10,18,19] deltorphins,[20] and the $\delta$-selective tetrapeptide JOM-13.[21] These $\beta$-methyl amino acids have side-chain groups that are biased in favor of one side-chain rotamer (Figure 1). This rotamer population bias leads to a less flexible side-chain group and allows for a more confident assessment of both peptide topography and analogue conformation−activity relationships.[22] This $\beta$-methylation yields an amino acid with only one $\alpha$ proton and one $\beta$ proton. Consequently, it is possible to determine which amino acid side-chain rotamer is most populated by use of COSY NMR spectroscopy and the Karplus correlation.[23] With knowledge of the side-chain group rotamer position one can determine the orientation of the aromatic substituent on the $\beta$ carbon and its relationship to the rest of the peptide. On the basis of these studies and biological activity assays, we will suggest interaromatic distances and relative orientations of the $\mu$ and $\delta$ opioid receptor aromatic pharmacophores that lead to the various types of pharmacological activities displayed by these peptides.

## Results and Discussion

**Structure−Activity Relationships.** As previously reported,[4,5] the cyclic parent peptide CTAP (**1**) displays high affinity for $\mu$ opioid receptors and very low affinity for $\delta$ receptors and is, therefore, quite selective. This peptide acts predominantly as a $\mu$ antagonist in vitro and in vivo. The replacement of the D-Phe residue in the amino terminal position with a $\beta$-MePhe residue of D configuration leads to analogues **2** ([(2*R*,3*R*)$\beta$-MePhe[1]]-CTAP) and **3** ([(2*R*,3*S*)$\beta$-MePhe[1]]CTAP). Both of these analogues are lower in affinity versus the $\mu$ receptor by about an order of magnitude, but with 4-fold to 5-fold higher affinity at the $\delta$ receptor than **1** (Table 1). Consequently, they are much less selective than the parent peptide **1**. Peptides **2** and **3** also differ from **1** in their in vitro biological activity profiles (Table 2) in that they are less than half as effective in shifting the dose−response curve of the known $\mu$ agonist PL-017. Moreover, both **2** and **3** differ from **1** in their MVD agonism. Analogue **2** has about twice the MVD agonism of **1**, whereas **3** has only about half the MVD agonism of **1** under the same assay conditions. Furthermore, **1** displays slight GPI agonism, whereas both **2** and **3** do not. Analogue **2** also displays twice as much antinociception (36%) in the tail-flick assay as **3** (Table 3). It should be noted that administration of these analogues led to behavior which indicates toxicity in several cases

**Table 1.** Rat Brain Opiate Receptor Binding Affinities of CTAP Analogues

| no. | analogue | $IC_{50}\mu$ (nM)[a] | $IC_{50}\delta$ (nM)[b] | $\delta/\mu$ |
|---|---|---|---|---|
| **1** | CTAP[c] | 2.1 (±0.3) | 5310(±280) | 2530 |
| **2** | [(2*R*,3*R*)β-MePhe$^1$] CTAP[d] | 20 (±5) | 1190 (±330) | 59 |
| **3** | [(2*R*,3*S*)β-MePhe$^1$] CTAP[d] | 21 (±3) | 1320 (±240) | 63 |
| **4** | [(2*S*,3*R*)β-MePhe$^1$] CTAP[d] | 5420 (±1020) | 13200 (±2470) | 2.43 |
| **5** | [(2*S*,3*S*)β-MePhe$^1$] CTAP[d] | 1500 (±670) | >15000 | >10 |
| **6** | [D-Tic$^1$]CTAP[e] | 1.2 (±0.2) | 1270 (±78) | 1060 |
| **7** | [D-Trp$^1$]CTAP | 1.39 (±0.37) | 3530 (±1440) | 2540 |
| **8** | [(2*R*,3*R*)β-MeTrp$^1$] CTAP | 18.7 (±4.1) | 3640 (±795) | 195 |
| **9** | [(2*R*,3*S*)β-MeTrp$^1$] CTAP[e] | 12.1 (±3.8) | 7480 (±1960) | 618 |
| **10** | [(2*S*,3*R*)β-MeTrp$^1$] CTAP[e] | 3400 (±400) | 7640 (±4800) | 2.2 |
| **11** | [(2*S*,3*S*)β-MeTrp$^1$] CTAP[e] | 1360 (±160) | 9180 (±1600) | 7.0 |
| **12** | [D-Tca$^1$] CTAP[e] | 173 (±135) | 211 (±65.5) | 1.2 |

[a] Versus [$^3$H]DAMGO. [b] Versus [$^3$H][D-Pen$^2$,4′-Cl-Phe$^4$,D-Pen$^5$]-enkephalin. [c] Data taken from ref 4. [d] Data taken from ref 7. [e] Data taken from ref 6.

(Table 3). There was a general occurrence of seizure, barrel rolls, circling, and in some cases, death. The frequency, severity, and duration of these phenomena were dose-dependent. At lower doses (6 nmol), tail-flick latency was not observable, and at higher doses (>30 nmol) toxicity-related behavior made testing of tail-flick latency impractical. So these data are presented with the caveat that loss of motor coordination may be erroneously ascribed to a change in tail-flick latency.

Substitutions with L-amino acids in the N-terminal position (i.e., [(2*S*,3*R*)β-MePhe$^1$]CTAP, **4**, and [(2*S*,3*S*)β-MePhe$^1$]CTAP, **5**) lead to analogues with dramatically reduced affinities for both the $\mu$ and $\delta$ receptor. This substitution evidently does not result in analogues that are inactive in the MVD and GPI assays, however. Analogue **5** exhibits MVD agonism to the same degree as **2**, but unlike **2**, does not act as a GPI antagonist (Table 2). Analogue **4** is the only β-MePhe analogue which acts essentially only as a $\mu$ agonist (Table 2), although a weak one. Analogue **5** has a similar antinociceptive potency as **2** as well as a similar activity in the MVD which suggests that their antinociceptive activities are due to their agonism at $\delta$ receptors despite low affinity for the $\delta$ receptor. Analogue **6** is in all respects very similar to the parent peptide. This peptide has a high affinity for the $\mu$ receptor and is very $\mu$ opiate receptor-selective (Table 1). This analogue also shifts the dose−response curve of PL-017 in the GPI assay (Table 2), but not that of DPDPE in the MVD assay (data not shown), and has little antinociceptive activity in the tail-flick assay (data not shown). The β-MePhe$^1$ analogues in this series lead to a variety of biological activities. Depending on which diastereoisomer is incorporated in the N-terminal position, the resultant analogue is a weak $\mu$ agonist (**4**), or a $\delta$ agonist (**5**), or a $\mu$ antagonist (**3**), or a simultaneous $\delta$ agonist/$\mu$ antagonist (**2**). These widely varying types of biological activities observed underscore the importance of the topographical arrangement of the aromatic pharmacophores in these analogues. Because the backbone is a stable template,[5] these various activities apparently result from differential side-chain group orientations.

CTAP analogues with D-Trp and β-methyl-tryptophan derivatives in the N-terminal position also were synthesized and characterized in vitro and in vivo (Tables 1 and 2). Some of their characteristics were strikingly similar to their Phe$^1$ counterparts. The most obvious case of this is seen in the $\mu$ receptor binding affinity data. Analogues which contain an amino acid of D configuration retain high affinity for the $\mu$ receptor. When D-Trp is substituted in position 1, the result is peptide **7** with opioid receptor binding characteristics similar to **1** (Table 1). This peptide, however, acts as a fairly potent, yet partial $\mu$ agonist in the GPI assay (Table 2) and is the most potent $\mu$ agonist CTAP analogue yet synthesized based on the GPI biological activity assay. It displays a 43% reduction in contraction at 1 $\mu$M concentration and an $EC_{50}$ of 37 nM (Table 2).

When conformationally constrained tryptophan analogues are substituted for D-Trp in the N-terminal position, some of the characteristics of the analogues change in a manner similar to those seen upon β-methyl substitution of phenylalanine, but others are unlike those seen in the phenylalanine derivatives. When D-Trp is substituted with β-methyltryptophans of D configuration (**8** and **9**, Table 1), the resulting analogues have their $\mu$ receptor affinity reduced about 10-fold (Table 1). This also is what is seen for the β-MePhe analogues. Unlike the β-MePhe analogues, the β-MeTrp analogues of D configuration do not have increased affinity for the $\delta$ receptor compared to CTAP, and as a result they are much more $\mu$ selective than their β-MePhe counterparts. When a β-MeTrp residue of L configuration is incorporated, peptides **10** and **11** are obtained, which have reduced affinities for both $\mu$ and $\delta$ receptors. Furthermore, the reductions in affinity for each receptor are very similar to the β-MePhe-containing peptides. These general similarities in receptor affinities, however, were not predictive of biological activities. The analogues with amino acids of D configuration did act as potent $\mu$ antagonists, with **9** showing the greatest GPI antagonist activity of any CTAP analogue reported thus far (Table 2). The $\mu$ antagonism of these analogues is somewhat surprising considering that the unbiased analogue **7** exhibits no $\mu$ antagonism but instead is a potent partial agonist at the $\mu$ receptor (Table 2). The analogues with L amino acids in position 1 are not potent $\mu$ antagonists, as is expected from their low affinity for the $\mu$ receptor. In this regard, analogues **10** and **11** are similar to **4** and **5**. When considering the agonist properties of the β-MeTrp-containing analogues, the outcome is inactivity. Only one β-MeTrp-containing analogue, **8**, shows even slight agonism at either receptor (Table 2), with agonism at the $\delta$ receptor only. It is arguable that the β-MeTrp-containing analogues are not appreciably different from their β-MePhe-containing counterparts. In two cases, the agonism is slight ($\delta$ activity of **3** and $\mu$ activity of **4**), and therefore a small total reduction would be viewed as inactivity (in β-MeTrp analogues **9** and **10**), and in another ($\delta$ activity of **2**) a small total reduction in agonism is still observable in the β-MeTrp analogue **8**. However, there is one clear difference in biological activity seen between the two classes (β-MeTrp$^1$ vs β-MePhe$^1$) even when the stereochemistry of the N-terminal amino acid is the same. Analogue **5** is a $\delta$ agonist of modest potency. Even considering an argument of generally reduced potency in β-MeTrp-containing peptides, one would still expect to see some activity in analogue **11**. This activity was not observed. When the data are taken as a whole, it is clear that the nature of the side-chain group moiety in position 1 is important in determining the binding affinity and

**Table 2.** Opioid Agonist and Antagonist Activities of CTAP Analogues

| no. | analogue | agonist activity at 1 $\mu$M (%) inhibition[a] MVD | agonist activity at 1 $\mu$M (%) inhibition[a] GPI | antagonism[b] PL-017 shift |
|---|---|---|---|---|
| **1** | CTAP[c] | 17 | 4 | 55 |
| **2** | [(2*R*,3*R*)$\beta$-MePhe$^1$] CTAP[d] | 34 | 0 | 19 |
| **3** | [(2*R*,3*S*)$\beta$-MePhe$^1$] CTAP[d] | 8 | 0 | 15 |
| **4** | [(2*S*,3*R*)$\beta$-MePhe$^1$] CTAP[d] | 0 | 13 | 1[e] |
| **5** | [(2*S*,3*S*)$\beta$-MePhe$^1$] CTAP[d] | 35 | 0 | 1 |
| **6** | [D-Tic$^1$]CTAP[c] | 10 ($\pm$2) | 1 | 60 ($\pm$15) |
| **7** | [D-Trp$^1$]CTAP | 13.6 ($\pm$3) | 43[f] | 1 |
| **8** | [(2*R*,3*R*)$\beta$-MeTrp$^1$] CTAP | 3.7 | 0 | 39 |
| **9** | [(2*R*,3*S*)$\beta$-MeTrp$^1$] CTAP | 0 | 0 | 68 |
| **10** | [(2*S*,3*R*)$\beta$-MeTrp$^1$] CTAP | 0 | 0 | 1 |
| **11** | [(2*S*,3*S*)$\beta$-MeTrp$^1$] CTAP | 0 | 0 | 2.6 |
| **12** | [D-Tca$^1$]CTAP[e] | 25 | 18 | 1.2 |

[a] Reported as the percent reduction in electrically evoked twitch height at a 1 $\mu$M concentration of the test peptide analogue. [b] Reported as the rightward fold-shift of the dose−response curve of the known agonist PL-017 (GPI, $\mu$) at a test peptide analogue concentration of 1 $\mu$M. [c] Data taken from ref 4. [d] Data taken from ref 7. [e] A PL-017 shift of 1-fold indicates no change in the dose−response curve. [f] Partial agonism ($E_{max}$ = 43%; $EC_{50}$ = 37 ($\pm$10) nM). [g] Data taken from ref 6.

**Table 3.** Percent Tail-Flick Latency Increases of CTAP Analogues[c]

| no. | analogue | minutes after injection 10 | 20 | 30 | 45 | 60 |
|---|---|---|---|---|---|---|
| **2** | [(2*R*,3*R*)$\beta$-MePhe$^1$] CTAP[b] | 4.3 ($\pm$1.5) | 27.6 ($\pm$5.5) | 36.1 ($\pm$5.1) | 24.4 ($\pm$4.2) | 5.8 ($\pm$4.2) |
| **3** | [(2*R*,3*S*)$\beta$-MePhe$^1$] CTAP[b] | 5.6 ($\pm$2.3) | 11.1 ($\pm$3.4) | 17.5 ($\pm$8.2) | 5.0 ($\pm$2.6) | 1.2 ($\pm$2.5) |
| **4** | [(2*S*,3*R*)$\beta$-MePhe$^1$] CTAP[b] | 6.1 ($\pm$2.9) | 13.9 ($\pm$3.1) | 20.2 ($\pm$6.6) | 10.8 ($\pm$7.0) | 4.0 ($\pm$4.6) |
| **5** | [(2*S*,3*S*)$\beta$-MePhe$^1$] CTAP[b] | 7.6 ($\pm$3.0) | 10.3 ($\pm$1.8) | 34.9 ($\pm$10.2) | 36.1 ($\pm$8.0) | 22.8 ($\pm$6.7) |
| **7** | [D-Trp$^1$]CTAP | 20.4 ($\pm$5.8) | 42.4 ($\pm$6.9) | 22.9 ($\pm$4.1) | 25.1 ($\pm$4.1) | 17.8 ($\pm$3.7) |
| **8** | [(2*R*,3*R*)$\beta$-MeTrp$^1$] CTAP | 30.6 ($\pm$3.6) | 41.2 ($\pm$5.9) | ND[c] | ND | ND |
| **9** | [(2*R*,3*S*)$\beta$-MeTrp$^1$] CTAP | 2.2 ($\pm$1.4) | −0.6 ($\pm$0.4) | 3.4 ($\pm$1.1) | ND | ND |
| **10** | [(2*S*,3*R*)$\beta$-MeTrp$^1$] CTAP | 4.0 ($\pm$2.2) | 5.3 ($\pm$2.3) | ND | ND | ND |
| **11** | [(2*S*,3*S*)$\beta$-MeTrp$^1$] CTAP | 45.9 ($\pm$5.8) | 39.8 ($\pm$6.1) | ND | ND | ND |
| **12** | [D-Tca$^1$]CTAP[d] | 22 | 57.2 | 72 | 65 | 68 |

[a] Data are presented as the percent increase in tail-flick latency. See METHODS for the equation used. [b] Data taken from ref 7. [c] ND indicates that tail-flick latency could not be determined due to evidence of toxicity-related behavior. [d] Data taken from ref 6.

biological activity of the peptide. In the case of amino acids with no conformational constraint, the receptor affinities are similar, but their activities vary widely. Analogue **1** acts predominantly as a $\mu$ antagonist, whereas **7** acts as a potent but partial $\mu$ agonist. In the case of peptides with a conformational bias, **5** acts as a $\delta$ agonist, whereas **11** is inactive. On the other hand, when the side-chain group is cyclized to confer near rigidity, the results are similar. Analogue **6** exhibits activity very similar to its linear analogue **1**—generally $\mu$ antagonism. Similarly, the side-chain cyclized amino acid-containing peptide **12** exhibits the same type of activity as its linear analogue **7**, namely, simultaneous weak agonism at both the $\mu$ and $\delta$ receptors.

Because these analogues are not particularly potent agonists, they do not necessarily provide particular insight for the topographical features required for opiate receptor activation. Nonetheless, these peptides do demonstrate that subtle changes in structure can have substantial effects on the type of activity displayed by the peptides (e.g., agonism vs antagonism). The important finding from this study is not that the peptides are potent, but rather that they show widely varying types of affinity and biological activity that are dictated by the nature of a conservative topographical structural modification. The parent peptide, CTAP, shows no $\mu$ agonism and little $\delta$ agonism, whereas the stereospecific addition of a single methyl group leads to peptides with improved agonism for $\mu$ (**4**, **7**) or $\delta$ (**2**, **5**) receptors. By understanding how these features lead to improved agonist activity, one can design new analogues which could be more capable of activating the opioid receptors.

**Conformational Analysis by Two-Dimensional NMR Spectroscopy and Molecular Modeling.** The conformations of analogues **2**−**5** and **7**−**11** were studied by NMR spectroscopy. Results of these NMR experiments and those performed previously on CTAP analogues[5,24] served for NMR-based molecular modeling of all 12 analogues. Complete assignment of all proton resonances was achieved using TOCSY, ROESY, and COSY experiments (Supporting Information). The chemical shift values are in good agreement with those reported previously for other CTAP analogues.[24] Proton chemical shifts also are in good agreement with values predicted for them based on published "typical" values for each residue in peptides.[25] Large deviations from typical amino acid residue proton chemical shift values are taken as evidence for atypical magnetic environments for them and as evidence for the presence of some chemical shift-inducing moiety, such as ring current effects from a neighboring aromatic moiety. The two-dimensional NMR experiments showed that these peptides adopt the same peptide backbone conformation as previously determined for other peptides in this series.[5,24] An upfield chemical shift was seen for the C$\beta$ and C$\delta$ protons of Arg$^5$. This fact, when taken with ROESY cross-peaks identifying through-space interactions of D-Trp$^4$ and Arg$^5$ residues, led to confirmation of the presence of a $\beta$II′-type turn with D-Trp$^4$ in the $i$+1 and Arg$^5$ in the $i$+2 "corner" positions. It is common

**Table 4.** Final Energy Miminization Values for CTAP Analogues (kJ/mol)[a]

| 1 | 2 | 3 | 4 | 5 | 6 | 7 | 8 | 9 | 10 | 11 | 12 |
|---|---|---|---|---|---|---|---|---|---|---|---|
| −350.31 (10) | −297.50(2) | −302.60(2) | −292.24 | −283.53 | −311.24 | −327.39 | −282.66 | −297.93 | −318.84(4) | −288.65 | −338.86 |
| −340.00 | −296.43 | −301.57 | −284.57 | −283.40 | −296.97 | −311.21 | −275.36 | −295.77 | −311.89 | −284.30 | −330.01 |
| −339.95 | −293.71 | −300.09(2) | −280.70 | −282.95 | −295.16 | −310.58 | −271.78 | −292.33 | −309.93 | −283.27 | −328.53 |
| −337.72(4) | −292.52(2) | −299.81 | −278.35 | −279.67(2) | −293.43(4) | −309.03 | −271.59 | −291.06 | −308.98 | −281.86 | −323.10 |
| −337.34(2) | −291.52 | −297.81 | −276.46 | −278.37(3) | −292.55 | −306.04 | −270.75 | −290.56 | −306.85 | −281.86 | −320.69(2) |
| −336.11 | −290.71 | −295.67 | −276.37 | −276.49 | −291.54(2) | −306.03 | −270.54 | −289.69 | −306.02 | −281.31 | −315.73(2) |
| −336.04 | −288.84(2) | −293.13 | −275.77 | −276.21 | −290.86(2) | −303.64 | −270.45 | −284.76 | −305.14(5) | −281.01 | −311.42 |
| −332.36 | −287.98 | −290.04(3) | −275.31 | −275.98 | −289.39 | −302.81 | −269.77 | −281.16 | −302.69 | −280.30 | −311.23 |
| −332.12 | −287.56(2) | −287.21 | −274.44 | −275.60 | −287.88 | −302.58 | −269.73 | −274.86 | −302.59 | −279.94 | −309.63 |
| −330.96 | −286.54(2) | −286.33 | −273.66 | −275.49(3) | −284.97 | −296.19 | −269.72 | −274.15 | −301.54 | −279.91 | −309.13(4) |
| −326.45 | −285.94 | −285.68(2) | −273.57 | −274.93(2) | −282.85 | −294.77 | −268.91 | −273.78 | −301.24 | −279.89 | −308.55 |
| −324.66 | −285.21 | −284.81 | −270.76 | −274.87 | −276.87 | −293.32 | −268.61 | −273.66 | −300.95 | −279.64 | −304.55 |
| −318.92 | −283.46 | −282.05(3) | −270.73 | −274.86 | −274.26 | −292.97 | −267.69 | −273.45 | −300.70(4) | −278.04 | −304.40(2) |
| | −283.05 | −281.81 | −270.64 | −271.95 | −271.17 | −292.64 | −267.40 | −273.29 | −300.67 | −277.17 | −304.05 |
| | −281.38 | −278.81 | −270.41 | −271.45 | −265.02 | −290.80 | −266.70 | −273.17 | −299.61 | −275.84 | −299.89 |
| | −281.27 | −276.44 | −270.33 | −270.69 | | −290.44 | −265.73 | −271.52 | −278.24 | −264.77 | −289.90 |
| | −280.41 | −261.45 | −270.30 | −268.23(2) | | −289.68(2) | −260.37 | −271.42 | | | −297.27 |
| | −278.44 | | −268.42 | −265.40 | | −289.51 | −257.68 | −265.44 | | | −290.02 |
| | −275.69 | | −268.29 | −255.88 | | −279.27 | −254.80 | −263.85 | | | −290.02 |
| | −275.47 | | −267.82 | | | −277.69 | −250.46 | −263.71 | | | |
| | −271.51 | | −267.67 | | | | −247.69 | −258.41 | | | |
| | | | −265.66 | | | | −236.89 | −248.84 | | | |
| | | | −261.37 | | | | | | | | |
| | | | −260.69 | | | | | | | | |
| | | | −259.18 | | | | | | | | |

[a] Numbers in parentheses represent the number of conformers that converged during minimization to the same structure.

for peptides to fold into a conformation where a D-amino acid residue adopts the $i+1$ position of a $\beta$-turn. Previous analyses using NMR and molecular dynamics simulations demonstrated that the CTAP peptide backbone is quite stable.[5,24] Therefore, a conservative amino acid side-chain group substitution (i.e., addition of a $\beta$-methyl group) can be made to an exocyclic amino acid residue which influences the topography of the peptide without drastically altering its peptide backbone conformation. Thus it is not surprising that the disulfide cyclic conformation remained the same in all of the analogues examined. Initial analogue conformations were based on these previous NMR and molecular dynamics simulations and were modified to reflect individual atypical proton chemical shift values and $^3J$ $H_\alpha-H_N$ and $^3J$ $H_\alpha-H_\beta$ coupling constants determined from DQF-COSY and COSY-35 experiments, respectively.

Analysis of the parent peptide **1** by molecular dynamics using NMR-derived restraints led to the identification of 13 distinct low energy conformations within 50 kJ/mol of the lowest energy conformer (see Table 4 for final energy values for each of the new analogues). While the conformations are folded slightly differently, each forms an arrangement where the D-Phe$^1$ → Tyr$^3$ interaromatic distance is approximately 7.4 Å. In this arrangement, the aromatic ring of the D-Phe$^1$ side-chain group points over the Cys$^2$ $\beta$ carbon. This feature is present in all CTAP analogues reported here that act as potent $\mu$ antagonists, and thus this is suggested to be in the "stereotypical" $\mu$ antagonist conformation. The conformation identified for **1** agrees in large part with the conformation proposed earlier.[5,24] A few differences have been identified, however. In the current study, it is clear that the amino acid side-chain groups of D-Trp$^4$ and Arg$^5$ are closer than that proposed by Kazmierski et al.[24] The affect of the D-Trp$^4$ aromatic ring is evident by the upfield shifting of the Arg$^5$ $\beta$ and $\gamma$ protons in comparison with typical values. Furthermore, ROE cross-peaks between the Arg$^5$ Cα proton and the Trp$^4$ H4 proton demonstrate a close proximity between the Arg$^5$ Cα proton and the D-Trp$^4$ H4 proton. Therefore, the D-Trp$^4$ side-chain group points away from the amino terminus and not in the same direction as the D-Phe$^1$ and Tyr$^3$ side-chain groups as suggested earlier. However, there was not an abundance of informative ROE cross-peaks. Typical ROE cross-peak patterns were evident in each of the analogues and were dominated by intraresidual cross-peaks and cross-peaks of the type CαH ($i$) → NH ($i+1$) and C$\beta$H ($i$)→ NH ($i+1$). The presence of a $\beta$II′ turn was also confirmed by the presence of an ROE cross-peak between the Arg$^5$ amide proton and the Thr$^6$ amide proton. Finally, several ROE cross-peaks were observed for interactions between C$\beta$ protons and intraresidual (H4 and H7) tryptophyl protons and the H2 protons of tyrosyl and phenylalanyl residues (see Supporting Information).

The other difference between the currently proposed conformation and that proposed by Kazmierski et al.[24] deals with the carboxy terminus. Previous analysis indicated that the carboxy terminus is near the amino-terminal portion of the peptide. The current analysis suggests that the carboxy terminus is more closely associated with the positively charged Arg$^5$ side-chain group. These modifications of the previously suggested conformation for **1** led to a conformation for CTAP that was lower in energy than the conformation previously suggested.

CTAP analogue **2** is interesting in that it is a potent $\mu$ antagonist with some $\delta$ agonist activity. This peptide exhibits its multiple opioid activity by virtue of its ability to adopt multiple low energy conformations (Figure 2). One low energy conformation resembles the stereotypical $\mu$ antagonist conformation—one in which the aromatic group of the amino-terminal residue is over the Cys$^2$ $\beta$ protons. In this case the interaromatic distance is 7.5 Å. In another low energy conformation this residue is closer to the Tyr$^3$ side-chain group. Here the two aromatic moieties are separated by <7.0 Å (Figure 2). Analogues of CTAP which have low energy conformations with this interaromatic distance demonstrate $\delta$ agonism as a rule. Analogue **3** is very similar to **2** in

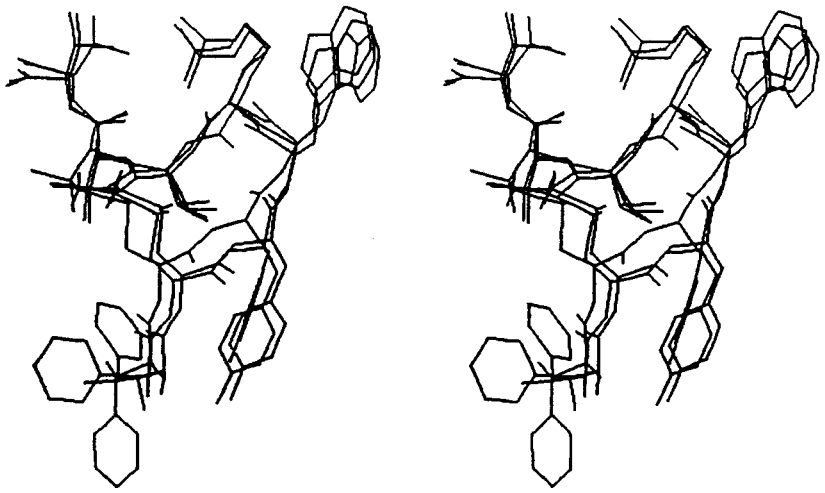

**Figure 2.** Stereoscopic view of three low energy conformers of **2**. The conformations shown are responsible for $\mu$ antagonism, $\delta$ agonism, and inactivity (see text).

structure. They differ only in the stereochemical arrangement of a $\beta$-methyl group in the amino terminal residue. This small change leads to a significant difference in biological activity. Unlike **2**, **3** is essentially a pure antagonist (<10% agonist inhibition at 1 $\mu$M) with very weak (8%, Table 2) agonist activity. In this analogue, the interaromatic distance is >7 Å for both of its low energy conformations—one of which is the typical $\mu$ antagonist arrangement. This suggests that the second low energy conformation is inactive and identifies the active conformation for $\delta$ agonism in analogue **2**. This means that the low energy conformation of **2** in which the phenyl ring of the amino terminal residue is pointing in the same direction as the Tyr$^3$ side-chain group phenol moiety is the conformation responsible for $\delta$ agonism. Analogue **4** is the only $\beta$-MePhe-containing peptide without both $\delta$ agonist activity and antagonist activity at the $\mu$ receptor (Table 2). This bioactivity can be explained by its low energy conformers. The amino terminal phenyl moiety is not positioned over the Cys$^2$ $\beta$ protons, but rather is over the Cys$^2$-Tyr$^3$ peptide bond in two of the three low energy conformations. In the third conformation, this aromatic moiety is in the region normally occupied by the Tyr$^3$ side-chain group. In this case, the Tyr$^3$ side-chain group adopts a different rotamer position, pointing generally toward the Arg$^5$ side-chain, and not toward the amino terminus, as is the case in the other analogues in this series. The energy minimized structure of analogue **5** has both position 1 and position 3 aromatic rings pointing toward the amino terminus. This arrangement is similar to that seen for one of the low energy conformations of analogue **2**, and it is similarly a $\delta$ agonist. In contrast with analogue **2**, however, the interaromatic distance in this peptide is 4.6 Å compared to a nearly 7 Å separation in **2**. While analogue **5** has relatively high agonist activity in the MVD, it has low affinity for the $\delta$ receptor. This may be due to a high efficacy of the analogue. Alternatively, it may be due to the activation of other pathways, the components being in the MVD but not in the purified $\delta$ receptor homogenate or which exist in different abundances, which lead to the observed effects. Other functional studies, such as the GTP$\gamma^{35}$S binding assay, might be able to distinguish between these possibilities.

When taken together, these four isomers of [$\beta$-MePhe$^1$]-CTAP reveal the criteria for opiate receptor activation in the CTAP series. It is clear that the $\mu$ antagonist activity is a result of a Tyr$^3$ side chain pointing toward the amino terminus and a $\beta$-MePhe$^1$ side-chain group pointing over the Cys$^2$ $\beta$ protons and an interaromatic distance of ≥7 Å. The $\delta$ agonist conformation consists of both $\beta$-MePhe$^1$ and Tyr$^3$ side-chain aromatic moieties pointing toward the amino terminus. In this case a wide range of interaromatic distances (4.6−7 Å) will suffice. This near overlap in interaromatic distances for $\mu$ antagonism and $\delta$ agonism (around 7 Å) may be responsible for the creation of multiply biologically active analogues such as **2**. These interaromatic distances identified as typical for $\mu$ antagonism are in excellent agreement with distances determined for peptides in the Dermorphin series (7.9−8.0 Å).[17] This 7.9 Å separation is seen in each of the low energy conformations of **6**, which adopts the typical conformation for $\mu$ antagonism and acts essentially as a pure $\mu$ antagonist (≤10% twitch-height reduction at 1 $\mu$M) with very weak if any $\delta$ agonist activity. In regards to $\mu$ opiate receptor affinity, selectivity, and $\mu$ opiate receptor antagonist potency, **6** is one of the best analogues characterized to date.

Analogue **7** is unique among the reported CTAP series peptides. This peptide is the only known high affinity partial agonist of the $\mu$ opiate receptor. Unlike the $\beta$-MePhe-containing peptides, this analogue is not conformationally biased toward one rotamer position for the amino terminal side-chain group. This lack of conformational constraint is seen in its 7.5 Hz $^3J$ $H_\alpha-H_\beta$ coupling constant, which indicates that this side-chain group is freely rotating about its $\alpha-\beta$ bond. This is unlike the $^3J$ $H_\alpha-H_\beta$ coupling constants of amino terminal $\beta$-methyl amino acids, which are greater than 11 Hz. Due to the flexibility of this analogue, it is difficult to ascribe a particular conformation to this peptide or to gauge accurately which conformation leads to $\mu$ agonism. However, the low energy conformation suggests that $\mu$ agonism may be the result of an arrangement in which both the D-Trp$^1$ and Tyr$^3$ side-chain group aromatic moieties point away from the amino terminus.

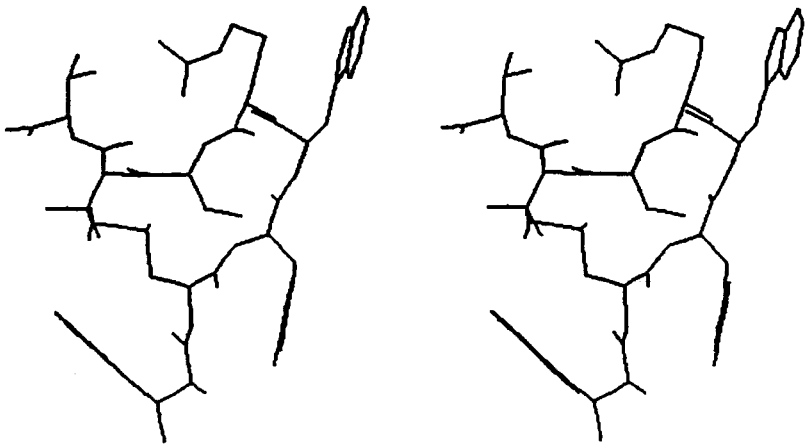

**Figure 3.** Stereoscopic view of the low energy conformation of **9**. This conformation shows the stereotypical arrangement of the aromatic pharmacophores that leads to $\mu$ antagonism.

The $\beta$-MeTrp-containing analogue **8** is very similar to its $\beta$-MePhe-containing counterpart **2**. They are both potent $\mu$ antagonists and exhibit measurable $\delta$ agonism. Like **2**, **8** adopts the stereotypical $\mu$ antagonist arrangement and has a >7 Å interaromatic separation (7.7 Å). Unlike **2**, however, the second low energy conformation of **8** does not have a <7 Å interaromatic distance (12.3 Å). This suggests that there may be more than one arrangement of the aromatic moieties of the first and third amino acid residue that is able to activate the $\delta$ receptor. In contrast, **9** is a pure $\mu$ antagonist, similar to its $\beta$-MePhe counterpart **3**, although **3** has some slight $\delta$ agonist activity. This peptide adopts the characteristic $\mu$ antagonist conformation (Figure 3). This conformation is especially stable in this analogue, as evidenced by the dramatic upfield shift of the $Cys^2$ $\beta$ protons. This peptide is the most potent $\mu$ antagonist synthesized to date, as determined by its ability to shift rightwardly the dose–response curve of the known $\mu$ agonist PL-017. Energy minimization of this peptide also offered evidence that the NMR constraints used in refining the structure were not changing an otherwise unsatisfactory initial conformation into an artificially low local energy minima. The structure obtained after energy minimization using NMR constraints converged with the energy minimized structure predicted prior to the NMR experiments. The interaromatic separation for this analogue is 7.3 Å. Analogues **10** and **11** are both essentially inactive at both the $\mu$ and $\delta$ opiate receptors, although **11** has some slight $\mu$ antagonist activity. Both analogues adopt low energy structures with aromatic separation and relative orientation similar to the conformations suggested to be responsible for the $\delta$ agonism seen in analogues **2** and **5**. The difference between **10** and **11**, when compared to **2** and **5**, is that the amino terminus is on the other face of the peptide ring structure. It is most likely that the unfavorable interaction between this terminal amine group and the $\delta$ receptor leads to these analogues' inactivity. Analogues **9**, **10**, and **11** also are interesting in that they exhibit no $\delta$ agonism, yet have some (albeit micromolar) affinity for the $\delta$ receptor. This may be explained by very low efficacy. Testing these analogues at even higher concentrations may reveal some very weak agonist activity. Analogue **12** has a cyclized amino acid in position 1, and hence it is unable to rotate freely around its $\alpha$–$\beta$ bond. This analogue is unusual in that it has similar weak binding affinity to $\mu$ and $\delta$ receptors as well as weak agonism of both receptors. The low energy conformation of this analogue explains its $\delta$ agonism. This peptide adopts a conformation similar to the one suggested as being responsible for the $\delta$ agonism of analogues **2** and **5**. The $\mu$ agonism of this peptide is surprising given its low energy conformation. However, a loss of interaction of the $Tyr^3$ side-chain group hydroxyl with the amino terminus would convert the conformation to the $\mu$ agonist conformation suggested for **7**. The side-chain cyclization in essence stabilizes the $\delta$ agonist topography at the expense of $\mu$ agonist arrangement (compare $\mu$ and $\delta$ agonist activities of **12** to **7**). In the low energy conformation, the interaromatic distance is 6.3 Å.

These 12 CTAP analogues show a remarkable variety of types of biological activities including partial $\mu$ agonism (**7**), $\mu$ antagonism (**1**, **3**, **6**, **8**, **9**), simultaneous $\mu$ and $\delta$ agonism (**12**), simultaneous $\mu$ antagonism and $\delta$ agonism (**2**), $\delta$ agonism (**5**), and inactivity (**4**, **10**, **11**). By comparing and contrasting the predicted low energy structures and the observed biological activities, it was possible to derive common characteristics responsible for agonist activity at the $\delta$ and $\mu$ receptor and antagonist activity at the $\mu$ receptor.

## Conclusions

Incorporation of aromatic $\beta$-methyl-containing amino acids into the amino terminal position of CTAP led to analogues of widely varying types of biological activity profiles. It is clear that an amino terminal residue of D configuration is a requirement for high affinity binding of the $\mu$ opiate receptor. Opiate receptor activation does not have this requirement. For $\mu$ opiate receptor activation, as evidenced by GPI agonism, analogue **4** was shown to have modest agonism, despite its >5 $\mu$M $IC_{50}$ for the receptor. The results are more striking when $\delta$ agonism, as seen in the MVD assay, is surveyed. The best example of this is analogue **5**, which reduces MVD twitch height by nearly 35%, despite a 15 $\mu$M $IC_{50}$ binding affinity for the receptor. The nature of the aromatic group in the amino terminal position (phenyl vs indole) is very important for receptor activation. Analogues **1** and **7** have practically identical receptor binding affinities and similar MVD ($\delta$) agonism. They differ dramatically in their ability to activate the $\mu$ receptor. At a 37 nM concentration, the D-Trp-containing peptide **7** exhibits >20% GPI twitch-height reduction,

whereas **1** is essentially inactive at 1 $\mu$M concentration. Another example includes a comparison of analogues **5** and **11**. Whereas **5** is the most potent $\delta$ agonist known in this series, **11** exhibits no detectable $\delta$ agonism up to a 1 $\mu$M concentration. Finally, a comparison of the cyclic amino acids $\alpha$ (D-Tic[1] and D-Tca[1]) reveals a cyclic phenylalanine (D-Tic[1])-containing peptide **6**, which has a little $\delta$ agonism and barely detectable $\mu$ agonism, whereas the cyclic tryptophan-containing (D-Tca[1]) peptide **12** is, in the CTAP series, the most potent simultaneous $\delta$ agonist/$\mu$ agonist known. Taken as two groups (peptides with $\beta$-MePhe in position 1 and peptides with $\beta$-MeTrp in position 1), the differences in activities become more obvious—peptides with $\beta$-MePhe include a simultaneous $\delta$ agonist/$\mu$ antagonist (**2**), a $\mu$ antagonist (**3**), a $\mu$ agonist (**4**), and a $\delta$ agonist (**5**), whereas peptides containing $\beta$-MeTrp display essentially only $\mu$ antagonism (**8**, **9**) or lack of activity (**10**, **11**).

The conformational characterization of these peptides was carried out in an effort to determine how peptides that are so similar in structure can elicit such varying biological responses. It was shown that the incorporation of the $\beta$-methyl group does have the intended affect. Namely, this methyl group, when placed on the $\beta$ carbon, will bias the rotamer population through steric effects toward a particular rotamer. This is evidenced by the high $^3J$ $H_\alpha-H_\beta$ coupling constants (>11 Hz) determined in the COSY-35 experiments. On the other hand, the coupling constant of the unbiased amino acid D-Trp[1] in analogue **7** was much lower (7.5 Hz), and indicated that it experienced free rotation about its $\alpha-\beta$ bond. The preferred conformation stabilizes certain interaromatic distances. By inspection of molecules with certain shared biological activities (e.g., $\delta$ agonism), suggestions can be made as to the structural features that lead to the activity. On the basis of the low energy conformations of these analogues and their known biological activities, aromatic pharmacophore arrangements are discovered for opiate receptor activity. Activation of the $\delta$ opiate receptor requires aromatic groups that are relatively close together (<7 Å) and both point in the same direction as the amino terminus. Antagonism of the $\mu$ receptor occurs when the aromatic groups are separated by >7 Å and the aromatic side-chain group of the amino terminal residue is pointing away from the amino terminus and toward the cysteine in the second position. Because there is a near overlap of the interaromatic distances around 7 Å and because some analogues adopt multiple low energy conformations, it is possible that some analogues will exhibit multiple activities when their interaromatic separation is near 7 Å. These structure—activity profiles suggest that it should be possible to make molecules that are simultaneously $\delta$ agonists and $\mu$ antagonists that take advantage of these pharmacophore arrangements and at the same time improve on other aspects of the drug such as bioavailability, efficacy, potency, selectivity, and affinity. These molecules could be potentially therapeutically useful in killing pain through $\delta$ agonism, yet avoid the unwanted side-effects that are typically associated with $\mu$ agonism.

## Experimental Section

**General Methods for Peptide Synthesis.** All peptides were synthesized in a stepwise fashion by solid-phase methods.[26] The solid support resin (1% DVB cross-linked pMBHA) and l-Pen(*S*-4′-methylbenzyl) were purchased from Peptides International (Louisville, KY). $N^\alpha$-Boc-protected D-Trp, D-Phe, L-Cys(*S*-4′-methylbenzyl), L-Tyr (*O*-2′,6′-dichlorobenzyl), l-Arg-($N^\gamma$-tosyl), and L-Thr(*O*-benzyl) were purchased from Bachem (Torrance, CA). Protected $\beta$-MeTrp and $\beta$-MePhe analogues suitable for solid-phase peptide synthesis were made according to procedures developed in this laboratory.[27−29] Tic and Tca were synthesized by published procedures.[30] These cyclized amino acids, $\beta$-methyl amino acids, and L-Pen(*S*-4′-methylbenzyl) were $N^\alpha$-t-Boc protected at their $\alpha$-amine group by literature methods.[31]

A 1 mmol scale was generally used, starting with 2.5 g of pMBHA resin (0.4 mequiv/g substitution, 100−200 mesh). The resin was swollen overnight in DMF and then washed with DCM, then DIEA, and then washed again in DCM. The carboxy terminal protected amino acid ($N^\alpha$-Boc-L-Thr(*O*-benzyl)) and subsequent $N^\alpha$-Boc-protected amino acids were coupled sequentially using an automated Milligen 9500 solid-phase peptide synthesizer, using DIC/HOBt as the coupling reagent for all amino acids except the amino terminal amino acids. The N-terminal amino acids were coupled using BOP/HOBt. The completeness of each coupling reaction was monitored by ninhydrin testing. After amino acid coupling the resin was washed with DMF and DCM, and then the $N^\alpha$-Boc group was removed with 48.5% TFA in DCM with 2.5% anisole as scavenger. The deblocked resin was then neutralized with DIEA in DCM. Subsequent washing with DCM made the resin ready for the next round of protected amino acid coupling. The amino acids were used in excess (with respect to the resin) during coupling (3-fold excess for DIC/HOBt coupling and 1.2-fold excess for BOP/HOBt coupling). After the N-terminal protected amino acid was coupled, the peptide-resin was $N^\alpha$-Boc deblocked with TFA, washed several times with DMF, and then several times with DCM. The resin was then dried under a nitrogen stream and dried overnight in vacuo. The peptide was then cleaved from the resin with concomitant amino acid side-chain group deprotection with anhydrous liquid HF (10 mL of HF per gram of dry peptide-resin) in the presence of *p*-cresol/p-thiocresol (1:1, v/v) as scavengers (1 mL of scavenger mixture per gram of dry peptide-resin). The HF cleavage reaction was performed at 0 °C for 1 h. The HF was then removed in vacuo and the resin washed in ether and extracted with glacial acetic acid. The extracted peptide was then frozen and lyophilized. This crude peptide was purified by RP-HPLC with a Vydac C-18 column using a gradient of 10−40% acetonitrile in 0.1% aqueous TFA. Fractions which contained pure peptide were pooled and lyophilized.

**General Method of Oxidation/Cyclization**. The peptide was cyclized by dissolving 100 mg of the purified linear peptide in 600 mL of $H_2O$/acetonitrile (2:1, v/v) and adding an excess of $K_3Fe(CN)_6$. The solution was maintained at a pH of 8.5 by dropwise addition of dilute $NH_4OH$ and was stirred for 2 h. The excess ferro- and ferri-cyanides were removed with Amberlite IRA-68 resin. The resin was then filtered and extracted with glacial acetic acid. The filtrate and the extract were then pooled and concentrated by rotary evaporation to give the crude cyclic peptide. This cyclic peptide was then purified by RP-HPLC using the method described above for the purification of the crude linear peptide. The purity of these peptides was assessed by TLC in four solvent systems and by analytical HPLC. In each case only one spot was observed by TLC, and by integration of HPLC chromatograms it was determined that each peptide was >98% pure. The identity of each peptide was confirmed by AAA, mass spectral $[M + H]^+$ molecular ion fragmentation pattern, and by two-dimensional NMR. Amino acid analyses were performed at the University of Arizona Biotechnology Core Facility using an Applied Biosystems model 420A amino acid analyzer with automatic hydrolysis (vapor phase at 160 °C for 100 mins using 6 N HCl) or with prior hydrolysis (6 N HCl, 110 °C, 24 h) and precolumn PTA-AA analysis. FAB-MS spectra were obtained from the College of Pharmacy at the University of Arizona. The analytical data for each analogue are given in Table 5.

**Table 5.** Analytical Data of CTAP Analogues[a]

| | | amino acid analysis | | | TLC[b] $R_f$ Values | | | | HPLC[c] | FAB-MS ($MH^+$) | |
|---|---|---|---|---|---|---|---|---|---|---|---|
| no. | analogue | Tyr(1) | Arg(1) | Thr(2) | A | B | C | D | K | calcd | obs |
| **2** | [(2*R*,3*R*)β-MePhe[1]] CTAP[d] | 1.00 | 1.09 | 1.86 | 0.746 | 0.760 | 0.427 | 0.585 | 2.32 | 1118 | 1118 |
| **3** | [(2*R*,3*S*)β-MePhe[1]] CTAP[d] | 1.00 | 1.08 | 2.14 | 0.711 | 0.744 | 0.427 | 0.585 | 2.13 | 1118 | 1118 |
| **4** | [(2*S*,3*R*)β-MePhe[1]] CTAP[d] | 1.00 | 1.02 | 2.14 | 0.711 | 0.744 | 0.393 | 0.560 | 1.39 | 1118 | 1118 |
| **5** | [(2*S*,3*S*)β-MePhe[1]] CTAP[b] | 1.00 | 1.08 | 2.00 | 0.724 | 0.744 | 0.385 | 0.551 | 1.48 | 1118 | 1118 |
| **7** | [D-Trp[1]]CTAP | 1.00 | 1.09 | 1.80 | 0.742 | 0.768 | 0.455 | 0.600 | 1.78 | 1143 | 1143 |
| **8** | [(2*R*,3*R*)β-MeTrp[1]] CTAP | 1.00 | 1.04 | 1.96 | 0.766 | 0.746 | 0.475 | 0.608 | 3.39 | 1157 | 1157 |
| **9** | [(2*R*,3*S*)β-MeTrp[1]] CTAP | 1.00 | 1.03 | 1.82 | 0.733 | 0.746 | 0.475 | 0.616 | 2.21 | 1157 | 1157 |
| **10** | [(2*S*,3*R*)β-MeTrp[1]] CTAP | 1.00 | 1.03 | 2.05 | 0.738 | 0.737 | 0.442 | 0.558 | 2.11 | 1157 | 1157 |
| **11** | [(2*S*,3*S*)β-MeTrp[1]] CTAP | 1.00 | 1.03 | 1.87 | 0.716 | 0.737 | 0.442 | 0.558 | 1.98 | 1157 | 1157 |

[a] Structures of all peptides were confirmed by one- and two-dimensional $^1$H NMR. [b] See General Methods. [c] Vydac 218TP104, 4.6 mm x 25 cm, Isocratic, 75% acetonitrile, 25% 0.1% TFA in $H_2O$; flow rate 1 mL/min; detection 230, 254, and 280 nm. [d] Data taken from ref 7.

**Amino Acid and Peptide Syntheses.** The four diastereoisomers of Nα-Boc-β-MeTrp(1′-Mes)[27] and the four diastereoisomers of Nα-Boc-β-MePhe[28,29] were synthesized according to published methods developed in this laboratory. D-Phe and D-Trp were cyclized using the Pictet−Spengler reaction[30] to generate D-Tic and D-Tca, respectively. D-Tic, D-Tca, the four Nα-Boc-β-MePhe isomers, the four Nα-Boc-β-MeTrp(1′-Mes) isomers, and L-Pen(*S*-4′-methylbenzyl) were Nα-t-Boc protected at their α-amine group using a published method.[31]

**CTAP (H-D-Phe-c[Cys-Tyr-D-Trp-Arg-Thr-Pen]-Thr-$NH_2$) (1).** This analogue was obtained by stepwise elongation of peptide-resin by the method outlined in the section on general peptide synthesis methods. Starting from 5 g of pMBHA resin, the following amino acids were added to the growing peptide chain: Nα-Boc-L-Thr(*O*-benzyl), Nα-Boc-L-Pen(*S*-4′-methylbenzyl), Nα-Boc-L-Thr(*O*-benzyl), Nα-Boc-L-Arg(Nγ-tosyl), Nα-Boc-D-Trp, Nα-Boc-L-Tyr(*O*-2′,6′-dichlorobenzyl), Nα-Boc-L-Cys(*S*-4′-methylbenzyl), and Nα-Boc-D-Phe. After the final amino acid was coupled, the terminal t-Boc group was removed with TFA and the resin washed several times with DMF, then several times with DCM, dried under a nitrogen stream, and dried additionally overnight in vacuo. Dry diethyl ether (50 mL) was added to the vessel containing the cleaved peptide and stirred for 20 min. The mixture was filtered and subject to several rounds of washing in diethyl ether (4 × 50 mL), vacuum-drying, and mechanical grinding with a spatula to break up clumping material. This product was then dried by vacuum filtration. The peptide was then extracted from the resin with glacial acetic acid (4 × 50 mL). The pooled extracts were then frozen and lyophilized (yield, 1.7 g). The crude linear peptide (500 mg) was then purified by RP-HPLC as described above to yield 293.3 mg of pure linear peptide. The pure linear peptide was then cyclized by the method described above and purified by RP-HPLC as described above to yield 188 mg of the pure cyclic disulfide peptide. See Table 5 for the analytical data of this peptide.

**[(2*R*,3*R*)β-MePhe[1]]CTAP (H-(2*R*,3*R*)β-MePhe-c[Cys-Tyr-D-Trp-Arg-Thr-Pen]-Thr-$NH_2$) (2).** This peptide was synthesized, cyclized, and purified according to the procedure described above, starting from 1.75 g of pMBHA resin. Yield of peptide-resin, 2.3 g; yield of crude linear peptide, 190 mg; yield of purified linear peptide, 110 mg; yield of purified cyclic disulfide peptide, 73 mg. See Table 5 for the analytical data of this peptide.

**[(2*R*,3*S*)β-MePhe[1]]CTAP (H-(2*R*,3*S*)β-MePhe-c[Cys-Tyr-D-Trp-Arg-Thr-Pen]-Thr-$NH_2$) (3).** This peptide was synthesized, cyclized, and purified according to the procedure described above, starting from 2.5 g of pMBHA resin. Yield of peptide-resin, 3.3 g; yield of crude linear peptide, 310 mg; yield of purified linear peptide, 220 mg; yield of purified cyclic disulfide peptide from 100 mg of purified linear peptide, 68 mg. See Table 5 for the analytical data of this peptide.

**[(2*S*,3*R*)β-MePhe[1]]CTAP (H-(2*S*,3*R*)β-MePhe-c[Cys-Tyr-D-Trp-Arg-Thr-Pen]-Thr-$NH_2$) (4).** This peptide was synthesized, cyclized, and purified according to the procedure described above, starting from 1.5 g of pMBHA resin. Yield of peptide-resin, 2.2 g; yield of crude linear peptide, 170 mg; yield of purified linear peptide, 120 mg; yield of purified cyclic disulfide peptide from 100 mg of purified linear peptide, 53 mg. See Table 5 for the analytical data of this peptide.

**[(2*S*,3*S*)β-MePhe[1]]CTAP (H-(2*S*,3*S*)β-MePhe-c[Cys-Tyr-D-Trp-Arg-Thr-Pen]-Thr-$NH_2$) (5).** This peptide was synthesized, cyclized, and purified according to the procedure described above, starting from 2.5 g of pMBHA resin. Yield of peptide-resin, 3.6 g; yield of crude linear peptide, 340 mg; yield of purified linear peptide, 210 mg; yield of purified cyclic disulfide peptide from 100 mg of purified linear peptide, 87 mg. See Table 5 for the analytical data of this peptide.

**[D-Tic[1]]CTAP (H-D-Tic-c[Cys-Tyr-D-Trp-Arg-Thr-Pen]-Thr-$NH_2$) (6).** This peptide was synthesized, cyclized, and purified according to the procedure described above, starting from 2.5 g of pMBHA resin. Yield of peptide-resin, 3.6 g; yield of crude linear peptide, 340 mg; yield of purified linear peptide, 210 mg; yield of purified cyclic disulfide peptide from 100 mg of purified linear peptide, 87 mg. See Table 5 for the analytical data of this peptide.

**[D-Trp[1]]CTAP (H-D-Trp-c[Cys-Tyr-D-Trp-Arg-Thr-Pen]-Thr-$NH_2$) (7).** This peptide was synthesized, cyclized, and purified according to the procedure described above, starting from 2.5 g of pMBHA resin. Yield of peptide-resin, 4.17 g; yield of crude linear peptide, 794.2 mg; yield of purified linear peptide from 500 mg of crude linear peptide, 284 mg; yield of purified cyclic disulfide peptide from 200 mg of purified linear peptide, 154.3 mg. See Table 5 for the analytical data of this peptide.

**[(2*R*,3*R*)β-MeTrp[1]]CTAP (H-(2*R*,3*R*)β-MeTrp-c[Cys-Tyr-D-Trp-Arg-Thr-Pen]-Thr-$NH_2$) (8).** This peptide was synthesized, cyclized, and purified according to the procedure described above, starting from 2.5 g of pMBHA resin. Yield of peptide-resin, 3.39 g; yield of crude linear peptide, 430.1 mg; yield of purified linear peptide, 143.3 mg; yield of purified cyclic disulfide peptide from 100 mg of purified linear peptide, 78.8 mg. See Table 5 for the analytical data of this peptide.

**[(2*R*,3*S*)β-MeTrp[1]]CTAP (H-(2*R*,3S*R*)β-MeTrp-c[Cys-Tyr-D-Trp-Arg-Thr-Pen]-Thr-$NH_2$) (9).** This peptide was synthesized, cyclized, and purified according to the procedure described above, starting from 2.5 g of pMBHA resin. Yield of peptide-resin, 3.19 g; yield of crude linear peptide, 390.7 mg; yield of purified linear peptide, 127.9 mg; yield of purified cyclic disulfide peptide from 100 mg of purified linear peptide, 72.4 mg. See Table 5 for the analytical data of this peptide.

**[(2*S*,3*R*)β-MeTrp[1]]CTAP (H-(2*S*,3*R*)β-MeTrp-c[Cys-Tyr-D-Trp-Arg-Thr-Pen]-Thr-$NH_2$) (10).** This peptide was synthesized, cyclized, and purified according to the procedure described above, starting from 2.5 g of pMBHA resin. Yield of peptide-resin, 3.41 g; yield of crude linear peptide, 411.1 mg; yield of purified linear peptide, 129.9 mg; yield of purified cyclic disulfide peptide from 100 mg of purified linear peptide, 68.4 mg. See Table 5 for the analytical data of this peptide.

**[(2*S*,3*S*)β-MeTrp[1]]CTAP (H-(2*S*,3*S*)β-MeTrp-c[Cys-Tyr-D-Trp-Arg-Thr-Pen]-Thr-$NH_2$) (11).** This peptide was synthesized, cyclized, and purified according to the procedure described above, starting from 2.5 g of pMBHA resin. Yield of peptide-resin, 3.44 g; yield of crude linear peptide, 386.4 mg;

yield of purified linear peptide, 137.2 mg; yield of purified cyclic disulfide peptide from 100 mg of purified linear peptide, 65.5 mg. See Table 5 for the analytical data of this peptide.

**[D-Tca[1]]CTAP (H-D-Tca-c[Cys-Tyr-D-Trp-Arg-Thr-Pen]-Thr-$NH_2$) (12).** This peptide was synthesized, cyclized, and purified according to the procedure described above, starting from 4 g of pMBHA resin. Yield of peptide-resin, 5.9 g; yield of crude linear peptide from 4 g of peptide-resin, 590 mg; yield of purified linear peptide, 228 mg; yield of purified cyclic disulfide peptide from 100 mg of purified linear peptide, 44 mg. See Table 5 for the analytical data of this peptide.

**MVD and GPI Bioassays.** Electrically induced smooth muscle contraction of mouse vas deferens (MVD) and strips of guinea pig ileum (GPI) longitudinal muscle-myenteric plexus was used for the bioassays. The smooth muscle assays were performed as described previously.[32,33] The GPI assay was performed by taking strips of longitudinal muscle-myenteric plexus from nonterminal ileum from male Hartley guinea pigs weighing 250−500 g. Tissues were suspended in organ baths (20 mL capacity) containing Krebs-bicarbonate buffer that was continuously bubbled with 95% $O_2$ and 5% $CO_2$ and maintained at 37 °C. The tissues were attached to isometric force transducers calibrated to 1 g of resting tension, and after 15 min equilibration period without tension they were stretched to 1 g of resting tension. The tissues were then transmurally stimulated between platinum electrodes at 0.1 Hz, 0.4 ms pulses, and supramaximal voltage. Contractions were recorded on a Grass 70 multichannel recorder. The effect of agonists on electrically evoked twitch tension was measured after incubation for 3 min. Antagonists were added to the bath 2 min before the addition of the agonist. Drugs were added in 14−60 $\mu$L volumes. Changes in contraction height after drug exposure were expressed as a percentage of the height average for a minute preceding delivery of the agonist divided by the contraction height at maximal inhibition after exposure to the dose of agonist. Agonist activities are reported as the percent inhibition of electrically evoked twitch height at a 1 $\mu$M concentration. Antagonism is represented by the dose−response curve rightward fold-shift after the addition of a 1 $\mu$M concentration of the antagonist. Standard errors are determined.

The MVD assay required the removal of vasa deferentia from male ICR mice (25−40 g) and placement in organ baths at 37 °C, which are oxygenated as above, in magnesium-free Krebs buffer. The tissues were hung without tension for 15 min, then placed under 0.5 g resting tension. The tissues were transmurally stimulated at 0.1 Hz, with 2 ms pulses and supramaximal voltage. Drug studies were performed as described for the GPI assays.

**Radioligand Binding Methods.** Receptor binding assays were performed essentially as previously described.[7] Membranes were prepared by taking whole brains from adult Sprague−Dawley rats (250−300 g) which were sacrificed by decapitation. The brain was rapidly removed and homogenized at 0 °C in 20 volumes of 50 mM Tris-HCl buffer at pH 7.4 using a glass-Teflon homogenizer. The membrane fraction resulting from a 15 min, 4 °C centrifugation at 48 000*g* was resuspended in 20 volumes Tris-HCl buffer and incubated at 25 °C to dissociate receptor from bound endogenous ligands. The incubated homogenate was then recentrifuged and resuspended in buffer.

For all inhibition studies, rat brain plasma membranes were incubated at 25 °C for 3 h in a total volume of 1 mL of 50 mM Tris-HCl, 1.0 mg/mL BSA, 30 $\mu$M bestatin, 50 $\mu$g/mL bacitracin, 10 $\mu$M captopril, and 0.1 mM phenylmethylsulfonyl fluoride buffer at pH 7.4 containing [$^3$H][4′-Cl-Phe$^4$]DPDPE (0.75 nM) or [$^3$H]DAMGO (1.0 nM), and at least 10 concentrations of each analogue. Each analogue was tested at least three times. Specific binding for the $\mu$ and $\delta$ receptors was defined as the difference in the amounts of radioligands bound in the absence and presence of 10 $\mu$M naltrexone.

Binding data were analyzed by a nonlinear least-squares regression analysis program (Inplot 4.03, GraphPad, San Diego, CA). Statistical comparisons between one-site and two-site fits were made using the *F*-ratio test using a *p* value of 0.05 as the cutoff for significance. Data best fitted by a one-site model were reanalyzed using the logistic equation. Data obtained from independent measurements are presented as the arithmetic mean ± SEM.

**In Vivo Assay Methods: Subjects.** Male ICR mice weighing 20−30 g were used throughout these studies. They were housed in groups of four in Plexiglas boxes, maintained in a light- and temperature-controlled environment with food and water provided ad libidum until antinociception testing was performed. All testing was in accordance with the recommendations and policies of the International Association for the Study of Pain (IASP) and National Institutes for Health (NIH) and the University of Arizona Guidelines for the care and use of laboratory animals.

**Antinociception Assay.** Antinociception determinations were made using the warm water tail-flick assay as described previously.[7] Water of 50 °C was used, and a 15 s cutoff time was employed. Antinociception was quantified from the test and control latencies to reflexive tail-flick by the relationship: % antinociception = (test − control)/(15 − control) × 100.

**Drug Administration.** The CTAP analogues were administered intracerebroventricularly to male ICR mice which were lightly ether-anesthetized. The drug was delivered by the method of Haley and McCormick.[34] Briefly, the skin covering the skull was split with a scalpel and the drug delivered via Hamilton microsyringe with a 25-gauge needle with a 2.5 mm depth-guard plastic collar attached. The drug was injected 2 mm caudal to bregma and 2 mm lateral to midline to ensure delivery to the lateral ventricle. Doses from 6 to 100 nmol per mouse were analyzed for antinociception and gross behavioral effects. Percent analgesia was determined for each dose at 10, 20, 30, 45, and 60 min postinjection.

**Statistics.** The values given in each of the in vitro and in vivo assays are given as the mean ± SEM.[35]

**NMR Experiments.** NMR samples were prepared by dissolving 5 mg of the dry, lyophilized, pure cyclic peptide in 500 $\mu$L of a 90% $H_2O$/10% $D_2O$ sodium acetate (50 mM) buffer containing sodium azide (1 mM) and were corrected to pH 4.5 with acetic acid-$d_3$ (final peptide concentration ~ 10 mM). For COSY-35 spectra, peptides were prepared identically, except the buffer contained no $H_2O$ (100% $D_2O$). Spectra were acquired without spinning at 303 K on a Bruker AM-500 spectrometer equipped with an Aspect 3000 computer and using a 5 mm water suppression probe. Resonance assignments were made by analysis of the two-dimensional DQF-COSY, TOCSY, and ROESY spectra. All 2D spectra were acquired in the phase-sensitive mode. Each spectrum was acquired using 2048 complex points in t2 and an F2 spectral width of 6250 Hz. Next, 750 real points were acquired in t1 with an F1 spectral width of 6250 Hz. The initial sampling delay was one dwell time, and the final t1 delay was 60 ms. At least 32 scans were collected per experiment. Solvent signal was suppressed by a phase-locked presaturation for 1.5 s at low power. Normal TOCSY and ROESY pulse sequences were followed by a Hahn-echo period to improve solvent suppression.[36] TOCSY spectra were acquired using the clean DIPSI-2RC TOCSY sequence.[37] ROESY spectra were acquired with a CW spin-lock field strength of 6670 Hz using a mixing time of 200 ms.

The generation of full 2D matrices was achieved by zero-filling to 2048 real points in t1 and right-shifting by one point in t1, multiplying by a sine-bell window function (ROESY) or a skewed sine-bell window function (TOCSY), and transforming into a 2048 × 1024 matrix. All 2D matrixes were created and analyzed using the FELIX95 computer program (Biosym Technologies, Inc., San Diego, CA) on a Silicon graphics workstation. The complete assignments and chemical shift data for the analogues examined (**2**, **3**, **4**, **5**, **7**, **8**, **9**, **10**, and **11**) are given in the Supporting Information.

**Molecular Modeling.** All theoretical conformational analyses were performed using the MacroModel molecular modeling package[38] (versions 4.0 and 4.5). MacroModel was executed from a Silicon Graphics IRIS workstation running the SGI

operating system AIX 4.0.5. The AMBER force field was used to calculate energy values using a distant-dependent dielectric constant ($\epsilon = 4$ D) and using the united-atom protocol and N-protonated forms. The starting conformation for these CTAP analogues was taken from the extensive NMR and molecular dynamics analyses reported previously for the parent peptide,[5,24] **1**, which showed the peptide backbone of this peptide to be conformationally stable. The conformations of these peptides were refined to reflect vicinal coupling constants determined from COSY spectra using the Karplus correlation,[23] ROE cross-peaks determined from ROESY spectra using correlation between signal strength and interatomic distance as reported in the literature,[39] and to reflect the changes in proton chemical shift values from typical values[25] seen in peptides that are due to anisotropic affects. A conformational grid search of 30° was then used for exocyclic rotatable bonds and conformers energy minimized. Conformations that were within 50 kJ/mol of the minimum-energy structure were grouped into families based on dihedral angle similarity and the lowest energy member of each family extensively minimized. Table 4 gives the results of these studies.

**Acknowledgment.** The authors thank Dr. Neil Jacobson for his help in obtaining NMR data and analysis. The authors thank Drs. Lakmal Boteju and Guigen Li for the syntheses of the four $N^{\alpha}$-Boc-$\beta$-MeTrp($N^{in}$Mes) and $N^{\alpha}$-Boc-$\beta$-MePhe analogues, respectively. This research was supported by a grant from the National Institute on Drug Abuse, NIDA grant number DA-06284. The contents of this paper are solely the responsibility of the authors and do not necessarily represent the official views of the National Institute on Drug Abuse.

**Supporting Information Available:** CTAP analogues, proton chemical shift assignment tables, and NOE/ROE data. This material is available free of charge via the Internet at http://pubs.acs.org.

## References

(1) Symbols and abbreviations are in accordance with the recommendations of the IUPAC−IUB Joint Commission on Biochemical Nomenclature: Nomenclature and Symbols for Amino Acids and Peptides. *Biochem. J.* **1984**, *219*, 345−373. Other abbreviations include the following: DCM, dichloromethane; DMF, dimethylformamide; HF, hydrogen fluoride; DIEA, diisopropylethylamine; MVD, mouse vas deferens; GPI, guinea pig ileum; SEM, standard error of the mean; FAB-MS, fast atom bombardment-mass spectroscopy; RP-HPLC, reversed-phase high performance liquid chromatography; AAA, amino acid analysis; BSA, bovine serum albumin; DIC, diisopropylcarbodiimide; TFA, trifluoroacetic acid; Tic, tetrahydroisoquinoline carboxylic acid; TCA, tetrahydo-$\beta$-carboline carboxylic acid; Boc, tertiary-butyloxycarbonyl; Pen, penicillamine; DVB, divinylbenzene; pMBHA, para-methylbenzhydrylamine; NMR, Nuclear Magnetic Resonance; DPDPE, c[D-Pen$^2$,D-Pen$^5$]enkephalin; PLO-17, H-Tyr-Pro-NMePhe-D-Pro-$NH_2$.

(2) Abdelhamid, E. E.; Sultana, M.; Portoghese, P. S.; Takemori, A. E. Selective Blockage of Delta Opioid Receptors Prevents the Development of Morphine Tolerance and Dependence in Mice. *J. Pharmacol. Exp. Ther.* **1991**, *258*, 299−303.

(3) Schiller, P. W.; Nguyen, T. M.-D.; Weltrowska, G.; Wilkes, B. C.; Marsden, B. J.; Lemieux, C.; Chung, N. N. Differential Stereochemical Requirements of $\mu$ vs. $\delta$ Opioid Receptors for Ligand Binding and Signal Transduction: Development of a Class of Potent and Highly $\delta$-Selective Peptide Antagonists. *Proc. Natl. Acad. Sci. U.S.A.* **1992**, *89*, 11871−11875.

(4) Kazmierski, W. M.; Wire, W. S.; Lui, G. K.; Knapp, R. J.; Shook, J. E.; Burks, T. F.; Yamamura, H. I.; Hruby, V. J. Design and Synthesis of Somatostatin Analogues with Topographic Properties that Lead to Highly Potent and Specific $\mu$ Opiate Receptor Antagonists with Greatly Reduced Binding at Somatostatin Receptors. *J. Med. Chem.* **1988**, *31*, 2170−2177.

(5) Kazmierski, W. M.; Yamamura, H. I.; Hruby, V. J. Topographic Design of Peptide Neurotransmitters and Hormones on Stable Backbone Templates: Relation of Conformation and Dynamics to Bioactivity. *J. Am. Chem. Soc.* **1991**, *113*, 2275−2283.

(6) Horan, J. H.; Wild, K. D.; Kazmierski, W. M.; Ferguson, R.; Hruby, V. J.; Weber, S. J.; Davis, T. P.; Fang, L.; Knapp, R. J.; Yamamura, H. I.; Kramer, T. H.; Burks, T. F.; Bowen, W. D.; Takemori, A. E.; Porreca, F. Unexpected Antinociceptive Potency of Cyclic [D-Tca$^1$]CTAP: Potential for a Novel Mechanism of Action. *Eur. J. Pharmacol.* **1993**, *233*, 53−62.

(7) Bonner, G. G.; Davis, P.; Stropova, D.; Ferguson, R.; Yamamura, H. I.; Porreca, F.; Hruby, V. J. Opioid Peptides: Simultaneous $\delta$ Agonism and $\mu$ Antagonism in Somatostatin Analogues. *Peptides* **1997**, *18*, 93−100.

(8) Sasaki, Y.; Chiba, T. Novel Deltorphin Heptapeptide Analogues with Potent Delta Agonist, Delta Antagonist, or Mixed Mu Antagonist/Delta Agonist Properties. *J. Med. Chem.* **1995**, *38*, 3995−3999.

(9) Qian, X.; Kövér, K. E.; Shenderovich, M. D.; Lou, B.-S.; Misicka, A.; Zalewska, T.; Horvath, R.; Davis, P.; Bilsky, E. J.; Porreca, F.; Yamamura, H. I.; Hruby, V. J. Newly Discovered Stereochemical Requirements in Side Chain Conformation of $\delta$ Opioid Agonists for Recognizing Opioid $\delta$ Receptors. *J. Med. Chem.* **1994**, *37*, 1746−1757.

(10) Qian, X.; Shenderovich, M. D.; Kövér, K. E.; Davis, P.; Horváth, R.; Zalewska, T.; Yamamura, H. I.; Porreca, F.; Hruby, V. J. Probing the Stereochemical Requirements for Receptor Recognition of $\delta$ Opioid Agonists Through Topographic Modifications in Position 1. *J. Am. Chem. Soc.* **1996**, *118*, 7280−7290.

(11) Chew, C.; Villar, H. O.; Loew, G. H. Characterization of the Bioactive Form and Molecular Determinants of Recognition of Cyclic Enkephalin Peptides at the $\delta$ Opiate Receptor. *Biopolymers* **1993**, *33*, 647−657.

(12) Froimowitz, M. Conformational Search in Enkephalin Analogues Containing a Disulfide Bond. *Biopolymers* **1990**, *30*, 1011−1025.

(13) Ohno, Y.; Segawa, M.; Ohishi, H.; Doi, M.; Kitamura, K.; Ishida, T.; Inoue, M.; Iwashita, T. Conformation of Deltorphin-II in Membrane Environments Studied by Two-Dimensional NMR Spectroscopy and Molecular Dynamics Calculations. *Eur. J. Biochem.* **1993**, *212*, 185−191.

(14) Nikiforovich, G. V.; Hruby, V. J.; Prakash, O.; Gehrig, C. A. Topographical Requirements for $\delta$ Selective Opioid Peptides. *Biopolymers* **1991**, *31*, 941−955.

(15) Flippen-Anderson, J. L.; Hruby, V. J.; Collins, N.; George, C.; Cudney, B. X-ray Structure of [D-Pen$^2$, D-Pen$^5$]enkephalin, a Highly Potent, $\delta$ Opioid Receptor-Selective Compound: Comparisons with Proposed Solution Conformations. *J. Am. Chem. Soc.* **1994**, *116*, 7523−7531.

(16) Loew, G.; Keys, C.; Luke, B.; Polgar, W.; Toll, L. Structure−Activity Studies of Morphiceptin Analogues: Receptor Binding and Molecular Determinants of $\mu$ Affinity and Selectivity. *Mol. Pharmacol.* **1986**, *29*, 546−553.

(17) Mierke, D. F.; Schiller, P. W.; Goodman, M. A Conformational Comparison of Two Stereoisomeric Cyclic Dermorphin Analogues Employing NMR and Computer Simulations. *Biopolymers* **1990**, *29*, 943−952.

(18) Hruby, V. J.; Toth, G.; Gehrig, C. A.; Kao, L. F.; Knapp, R.; Lui, G. K.; Yamamura, H. I.; Kramer, T. H.; Davis, P.; Burks, T. F. Topographically Designed Analogues of [D-Pen$^2$, D-Pen$^5$]enkephalin. *J. Med. Chem.* **1991**, *34*, 1823−1830.

(19) Toth, G.; Russell, K. C.; Landis, G.; Kramer, T. F.; Fang, L.; Knapp, R.; Davis, P.; Burks, T. F.; Yamamura, H. I.; Hruby, V. J. Ring Substituted and Other Conformationally Constrained Tyrosine Analogues of [D-Pen$^2$, D-Pen$^5$]enkephalin with Delta Opioid Receptor Selectivity. *J. Med. Chem.* **1992**, *26*, 2384−2391.

(20) Peter, A.; Toth, G.; Olajos, E.; Tourwe, D. Chromatographic Behavior of Opioid Peptides Containing $\beta$-Methylphenylalanine Isomers. *J. Chromatogr.* **1995**, *A 705*, 267−273.

(21) Mosberg, H. I.; Omnaas, J. R.; Lomize, A. Heyl, D. L.; Nordan, I.; Mousigian, C.; Davis, P.; Porreca, F. Development of a Model for the Delta Opioid Receptor Pharmacophore. 2. Conformationally, Restricted Phe$^3$ Replacements in the Cyclic Delta Receptor Selective Tetrapeptide Tyr-c[D-Cys-Phe-D-Pen]OH (JOM-13). *J. Med. Chem.* **1994**, *37*, 4384−4391.

(22) Hruby, V. J.; Li, G.; Haskell-Luevano, C.; Shenderovich, M. Design of Peptides, Proteins and Peptidomimetics in Chi Space. *Biopolymers* **1997**, 43, 219−266.

(23) Karplus, M. Contact Electron-Spin Coupling of Nuclear Magnetic Moments. *J. Phys. Chem.* **1959**, *30*, 11−15.

(24) Kazmierski, W. M.; Ferguson, R. D.; Lipkowski, A. W.; Hruby, V. J. A Topographical Model of $\mu$-Opioid and Brain Somatostatin Receptor Selective Ligands. *Int. J. Pept. Protein Res.* **1995**, *46*, 265−278.

(25) Bundi, A.; Wüthrich, K. $^1$H NMR Parameters of the Common Amino Acid Residues Measured in Aqueous Solution of the Linear Peptides H-Gly-Gly-X-L-Ala-OH. *Biopolymers* **1979**, *18*, 285−297.

(26) Upson, D. A.; Hruby, V. J. Synthesis of Specifically Deuterated S−Benzylcysteines and of Oxytocin and Related Diastereomers Deutereated in the Half-cystine Positions. *J. Org. Chem.* **1976**, *41*, 1353−1358.

(27) Boteju, L. W.; Wegner, K.; Qian, X.; Hruby, V. J. Asymmetric Synthesis of Unusual Amino Acids: Synthesis of Optically Pure Isomers of N-Indole-(2-mesitylenesulfonyl)-$\beta$-methyltryptophan. *Tetrahedron* **1994**, *50*, 2391−2404.
(28) Dharanipragada, R.; Nicolas, E.; Töth, G.; Hruby, V. J. Asymmetric Synthesis of Unusual Amino Acids: Synthesis of Optically Pure Isomers of Beta-Methylphenylalanine. *Tetrahedron Lett.* **1989**, *30*, 6841−6844.
(29) Li, G.; Jarosinski, M. A.; Hruby, V. J. Diastereospecific Tandem Michael-like Addition/Electrophilic Bromination: A One-pot Tandem Asymmetric Synthesis of Precursors of Unusual Amino Acids. *Tetrahedron Lett.* **1993**, *34*, 2561−2564.
(30) Pictet, A.; Spengler, T. Uberdie Bildung von Isochinolin-Derivaten durch Einworking von Methylal auf Phenyl-athylamine und Tyrosin. *Chem. Ber.* **1911**, *44*, 2030−2036.
(31) Tarbell, D. S.; Yamamoto, Y.; Pope, B. M. New Method to Prepare *N*-*tert*-butoxycarbonyl Derivatives and the Corresponding Sulfur Analogues from Di-*tert*-butyl Dicarbonate or Di-*tert*-butyl Dithiolodicarbonates and Amino Acids. *Proc. Natl. Acad. Sci. U.S.A.* **1972**, *69*, 730−732.
(32) Hughes, J.; Kosterlitz, W.; Leslie, F. M. Effect of Morphine on Adrenergic Transmission in the Mouse Vas Deferens: Assessment of Agonist and Antagonist Potencies of Narcotic Analgesics. *Br. J. Pharmacol.* **1975**, *53*, 371−381.
(33) Kosterlitz, H. W.; Lydon, R. J.; Wat, A. J. The Effects of Adrenaline, Noradrenaline, and Isoprenaline on Inhibitory alpha- and beta-Adrenoceptors in the Longitudinal Muscle of the Guinea Pig Ileum. *Br. J. Pharmacol.* **1970**, *39*, 398−413.
(34) Haley, T. J.; McCormick, W. G. Pharmacological Effects Produced by Intracerebral Injections of Drugs in the Conscious Mouse. *Br. J. Pharmacol. Chem.* **1957**, *12*, 12−15.
(35) Tallarida, R. J.; Murray, R. B. *Manual of Pharmacological Calculations with Computer Programs*, 2nd ed.; Springer-Verlag: New York, 1987, pp 26−31.
(36) Rance, M.; Sorensen, O. W.; Bodenhausen, G.; Wagner, G.; Ernst, R. R.; Wüthrich, K. Improved Spectral Resolution in COSY $^1$H NMR Spectra of Proteins *via* Double Quantum Filtering. *Biochem. Biophys. Res. Commun.* **1983**, *117*, 479−485.
(37) Cavanaugh, J.; Rance, M. Suppression of Cross-Relaxation Effects in TOCSY Spectra via a Modified DIPSI-2 Mixing Sequence. *J. Magn. Res.* **1992**, *96*, 670−678.
(38) Mohamadi, F.; Richards, N. G. J.; Guida, W. C.; Liskamp, R.; Lipton, M.; Caufield, C.; Chang, G.; Hendrickson, T.; Still, W. C. Macromodel − An Integrated Software System for Modeling Organic and Bioorganic Molecules Using Molecular Mechanics. *J. Comput. Chem.* **1990**, *11*, 440−467.
(39) Polinsky, A.; Cooney, M. G.; Toy-Palmer, A.; Osapay, G.; Goodman, M. Synthesis and Conformational Properties of the Lanthionine Bridged Opioid Peptide [D-Ala$^2$, Ala$^5$]enkephalin as Determined by NMR and Computer Simulations. *J. Med. Chem.* **1992**, *35*, 4185−4194.

JM9900218